

# Facile Combustion Synthesis of ZnFe<sub>2</sub>O<sub>4</sub> for Photocatalytic Oxidative Desulfurization of Thiophene in Model Oil

Rui-Hong Liu and Fa-Tang Li\*

College of Science, Hebei University of Science and Technology, Shijiazhuang, 050018 China

**Abstract:** Nano-ZnFe<sub>2</sub>O<sub>4</sub> photocatalysts are one-step synthesized via solution combustion route, which are characterized by XRD, TEM, and UV-vis DRS. The photocatalytic activity of these samples are evaluated by the removal of thiophene in model oil under visible light irradiation. The influences of fuel amount on the particle size and photocatalytic performance of the as-synthesized catalysts are investigated. The results show that the ZnFe<sub>2</sub>O<sub>4</sub> with the particle size of 21.9 nm exhibits the highest photocatalytic ability, which is acquired using triethylamine hydrochloride as fuel in the fuel-rich combustion condition. The desulfurization yield of model oil can reach 92.5% in 5 h photo-irradiation and the sulfur content can be decreased from 200 ppm to 15 ppm.

**Keywords:** Combustion synthesis, ZnFe<sub>2</sub>O<sub>4</sub>, photocatalytic desulfurization, thiophene.

## 1. INTRODUCTION

Sulfur-containing compounds in fuel oils would not only convert to sulfur oxide (SO<sub>x</sub>) during combustion resulting in acid rain and serious haze, but also make the catalysts to be poisoned in emission control systems [1]. Therefore, to protect environment against contamination, desulfurization from fuel oils has become an increasingly global research topic. Conventional catalytic hydrodesulfurization (HDS) has been effectively used to remove thiols, sulfides, and disulfides from fuels [2]. However, HDS requires high temperature, high pressure and even expensive hydrogen consumption [3], which leads to the high operation cost. Meanwhile, HDS is less efficient in thiophenes and their derivatives because of the steric hindrance [4].

Alternatively, photocatalytic oxidation desulfurization technique, recognized as a effective desulfurization method because of its high oxidative ability and low cost, has received increasing widespread interest [5-7]. To reach the practical application of photocatalysis, the development of inexpensive photocatalysts is a prerequisite. It is known that both Zn and Al are abundant elements in the earth, which makes the compound of ZnFe<sub>2</sub>O<sub>4</sub> to be a cheap material. On the other hand, ZnFe<sub>2</sub>O<sub>4</sub> has a narrow band gap from 1.6 to 2.0 eV [8], which endows ZnFe<sub>2</sub>O<sub>4</sub> ability of visible light absorption.

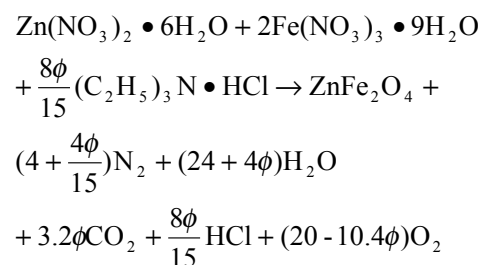
Solution combustion synthesis is a time- and energy-saving technology in preparing nanomaterials [9]. In this research, nano-ZnFe<sub>2</sub>O<sub>4</sub> powders are facile

synthesized *via* solution combustion route and their photocatalytic activity in desulfurization of thiophene are investigated. The preparation of inexpensive ZnFe<sub>2</sub>O<sub>4</sub> *via* one-step route and its application in sulfur removal of model oil would provide reference for the production of clean oils.

## 2. EXPERIMENTAL

### 2.1. Preparation of ZnFe<sub>2</sub>O<sub>4</sub> Photocatalysts

All chemicals were acquired from Sinopharm Group Co. Ltd. (Shanghai, China) and used as received without further purification. To prepare ZnFe<sub>2</sub>O<sub>4</sub>, 0.010 mol of Zn(NO<sub>3</sub>)<sub>2</sub>·6H<sub>2</sub>O and 0.020 mol of Fe(NO<sub>3</sub>)<sub>3</sub>·9H<sub>2</sub>O was mixed with various amount of triethylamine hydrochloride ((C<sub>2</sub>H<sub>5</sub>)<sub>3</sub>N·HCl) under continuously heating on an electric furnace until a white solution formed. Afterwards, the solution would burn and lots of gas emitted. Finally, the residual powders were collected and ground to obtain ZnFe<sub>2</sub>O<sub>4</sub> sample. The potential combustion reactions are proposed as follows according to the Jain's proposal [10].



Where  $\phi$  represents fuel/oxidizer ratio. The mixture is stoichiometric when  $\phi = 1$ , fuel lean when  $\phi > 1$  and fuel rich when  $\phi < 1$ . The samples were labeled from ZF0.8 to ZF1.4 when  $\phi$  is taken as 0.8-1.4, respectively, as shown in Table 1.

\*Address correspondence to this author at the College of Science, Hebei University of Science and Technology, Shijiazhuang, 050018, China; Tel: +86-311-8166971; Fax: +86-311-81668528; E-mail: lifatang@126.com

**Table 1:  $\phi$  Value and Crystalline Size of Various Samples**

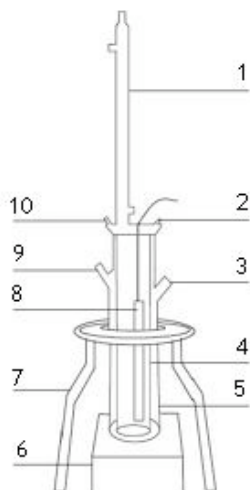
$\phi$ Value	Sample	Crystalline size (nm)
0.8	ZF0.8	21.0nm
1.0	ZF1.0	25.4nm
1.2	ZF1.2	21.9nm
1.4	ZF1.4	18.6nm

## 2.2. Characterization of Samples

X-ray diffraction (XRD) analysis was carried out on a Rigaku D/MAX 2500 X-ray diffractometer. High-resolution transmission electron microscopy (HRTEM) images were obtained using JEOL JEM-2100 electron microscope. The photo-absorption properties of the photocatalysts were observed by UV-Vis diffuse reflectance spectra (DRS) on a Thermo Scientific Evolution 220 spectrophotometer.

## 2.3. Photocatalytic Oxidation Desulfurization

The photocatalytic oxidation reaction was conducted in an XPA-II photochemical reactor (Nanjing Xujiang Electromechanical Factory), which is shown in Scheme 1. 17.7 $\mu\text{L}$  of thiophene was dissolved in 50 mL of n-octane to form model diesel oil with sulfur content of 200 ppm ( $\mu\text{g/g}$ ). The oil was mixed vigorously with 50 mL water and the mixture was visible-light irradiated in the presence of 0.05g photocatalyst using 300W Xe lamp equipped 420 nm filter as light source. To determine the initial and residual sulfur content, liquid samples were withdrawn from the reactor at fixed time intervals and measured using an ultraviolet fluorescence sulfur analyzer and then desulfurization yield could be calculated accordingly.

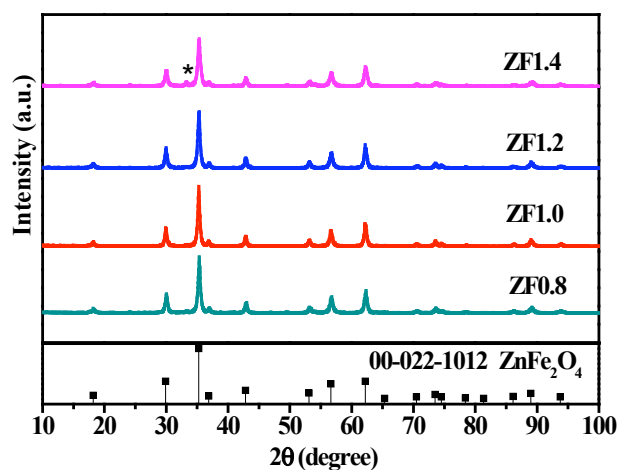
**Scheme 1:** Schematic diagram of experimental apparatus.

1-condenser tube; 2- inlet of water; 3- inlet of air; 4- silicon cold trap; 5- glass reactor; 6- magnetic stirrer; 7- bracket of reactor; 8- Hg lamp; 9- outlet of air; 10- outlet of water

## 3. RESULTS AND DISCUSSION

### 3.1. XRD Patterns

XRD patterns of the samples are shown in Figure 1. It is seen that the diffraction peaks of almost all the samples are good agreement with its franklinite phase (JCPDS No. 00-022-1012) except a very weak peak at  $33.1^\circ$  in ZF1.4 that is attributed to  $\text{Fe}_2\text{O}_3$ . Possible impurities such as  $\text{Fe}_2\text{O}_3$  or  $\text{ZnO}$  cannot be detected in other samples, indicating the complete combustion. Using the Scherrer formula:  $D = K\lambda/\beta\cos\theta$  [11], where  $K$  is a constant of 0.89,  $\lambda = 0.15148$  nm,  $\theta =$  Bragg angle,  $\beta =$  full width at half maximum (FWHM), mean crystallite size ( $D$ ) is estimated from the FWHM of the (311) diffraction peak at  $35.26^\circ$   $2\theta$  degree of the samples. The crystallite size results are shown in Table 1. It is seen that the crystalline size of  $\text{ZnFe}_2\text{O}_4$  becomes larger firstly and then smaller with the increase of fuel, which is related to the combustion temperature. It is known that less fuel would lead to the lower temperature, whereas excessive fuel would also result in the incomplete combustion and thus the lower temperature. Therefore, when  $\phi = 1$  the combustion temperature reaches the highest and the crystalline size is the largest.

**Figure 1:** XRD patterns of the samples.

### 3.2. TEM and HRTEM Images

Figure 2 shows the TEM and HRTEM images of sample ZF1.2. From Figure 2a it is seen that the sizes of the particles are uniform with diameters of

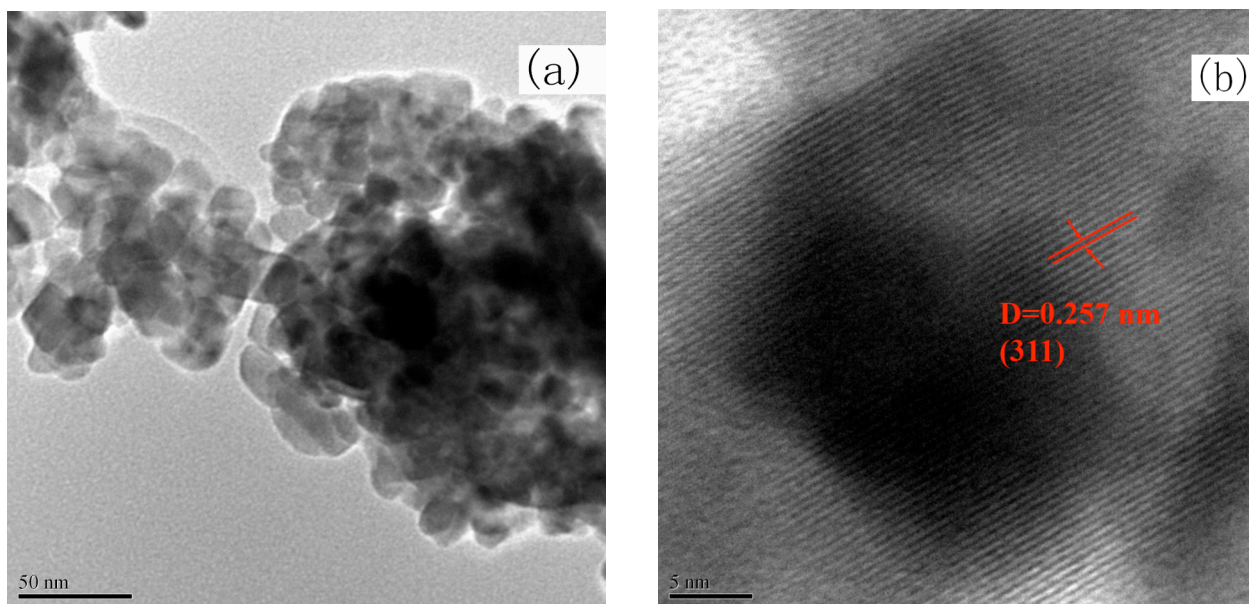


Figure 2: (a) TEM and (b) HRTEM images of sample ZF1.2

approximate 20 nm, which is consistent with the calculated XRD results. The uniform sizes are ascribed to the homogeneous mixture of precursor in the atomic level. From the HRTEM image shown in Figure 2b it can be seen that the interplanar spacing is 0.257 nm. This value corresponds to the (311) plane of  $\text{ZnFe}_2\text{O}_4$ , further confirming its existence.

### 3.3. Optical Absorption Performance

To observe the photo-absorption ability of the samples, UV-Vis DRS were conducted, which are shown in Figure 3. It can be seen that the as-prepared  $\text{ZnFe}_2\text{O}_4$  samples exhibit light absorption ability in visible-light region. The absorption thresholds are at around 677 nm, corresponding to a band gap of 1.83

eV using the equation of  $E_g = 1240/\lambda$ , which is close to the reported value of 1.82 eV. Such narrow band gap would provide foundation for the excellent photo-absorption and the photocatalytic activity.

### 3.4. Photocatalytic Activity in Desulfurization

Figure 4 shows the photocatalytic degradation efficiency of thiophene in the presence of various photocatalysts under the illumination of Xe lamp. Photocatalytic sulfur removal of thiophene in 5 h is 92.5%, 90.6%, 84.5%, and 79.2% when the employed photocatalysts are ZF1.2, ZF1.4, ZF0.8, and ZF1.0, respectively, showing ZF1.2 has the highest photocatalytic activity because ZF1.2 has appropriate crystallinity degree and crystalline size.

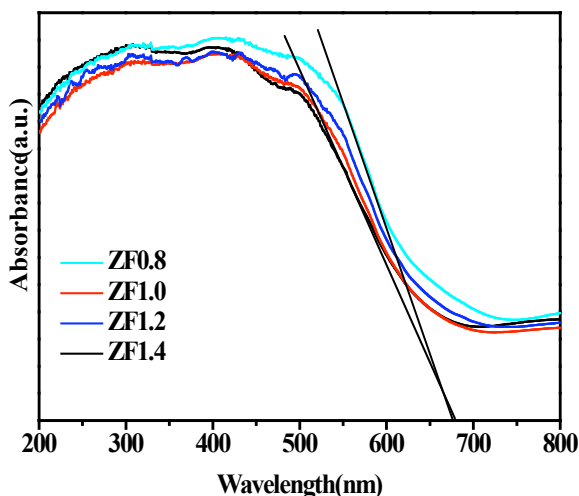


Figure 3: UV-Vis DRS of all the  $\text{ZnFe}_2\text{O}_4$  samples.

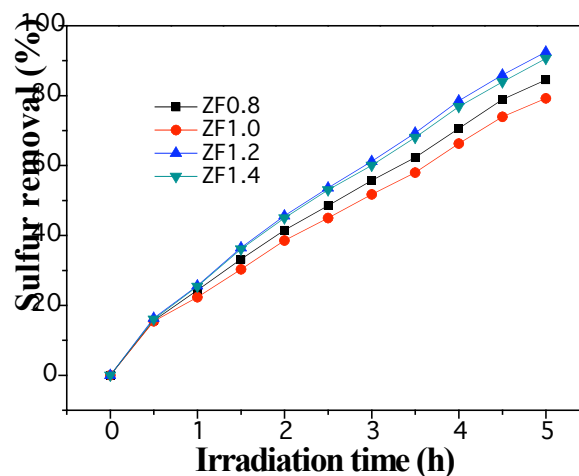


Figure 4: Time-course variation of sulfur removal of thiophene over different photocatalysts.

## CONCLUSIONS

The ZnFe<sub>2</sub>O<sub>4</sub> nano-powders are successfully synthesized *via* facile solution combustion route. The desulfurization process of thiophene in the presence of ZnFe<sub>2</sub>O<sub>4</sub> photocatalysts has been investigated. The sample prepared using 0.010 mol of Zn(NO<sub>3</sub>)<sub>2</sub>·6H<sub>2</sub>O, 0.020 mol of Fe(NO<sub>3</sub>)<sub>3</sub>·9H<sub>2</sub>O and 0.0064 mol of (C<sub>2</sub>H<sub>5</sub>)<sub>3</sub>N·HCl exhibited the highest desulfurization ability. The sulfur content can be depressed from 200 ppm to 15 ppm in 5 h under visible light irradiation.

## ACKNOWLEDGEMENTS

We thank National Natural Science Foundation of China (21376061) for the financial support.

## REFERENCES

- [1] Zeng XY, Xiao XY, Li Y, Chen JY and Wang HL. Deep desulfurization of liquid fuels with molecular oxygen through graphene photocatalytic oxidation. *Appl Catal B: Environ* 2017; 209: 98-109. <http://dx.doi.org/10.1016/j.apcatb.2017.02.077>
- [2] Li FT, Kou CG, Sun ZM, Hao YJ, Liu RH, *et al.* Deep extractive and oxidative desulfurization of dibenzothiophene with C<sub>5</sub>H<sub>9</sub>NO·SnCl<sub>2</sub> coordinated ionic liquid. *J Hazard Mater* 2012; 205-206: 164-170. <http://dx.doi.org/10.1016/j.jhazmat.2011.12.054>
- [3] Li XZ, Zhu W, Lu XW, Zuo SX, Yao C, *et al.* Integrated nanostructures of CeO<sub>2</sub>/attapulgite/g-C<sub>3</sub>N<sub>4</sub> as efficient catalyst for photocatalytic desulfurization: Mechanism, kinetics and influencing factors. *Chem. Eng J* 2017; 326: 87-98. <http://dx.doi.org/10.1016/j.cej.2017.05.131>
- [4] Ko NH, Lee JS, Huh ES, Lee H, Jung KD, *et al.* Extractive desulfurization using Fe-containing ionic liquids. *Energy Fuels* 2008; 22: 1687-1690. <http://dx.doi.org/10.1021/ef7007369>
- [5] Liu RH and Li FT. Photocatalytic oxidation kinetics for desulfurization of dibenzothiophene with Al<sub>2</sub>O<sub>3</sub>/g-C<sub>3</sub>N<sub>4</sub> heterojunction. *International Journal of Petroleum Technology* 2014, 1: 33-36. <http://dx.doi.org/10.15377/2409-787X.2014.01.02.1>
- [6] Li FT, Liu Y, Sun ZM, Zhao Y, Liu RH, *et al.* Photocatalytic oxidative desulfurization of dibenzothiophene under simulated sunlight irradiation with mixed-phase Fe<sub>2</sub>O<sub>3</sub> prepared by solution combustion. *Catal Sci Technol* 2012; 2: 1455-1462. <http://dx.doi.org/10.1039/c2cy00485b>
- [7] Li XZ, Li FH, Lu XW, Zuo SX, Yao C, *et al.* Development of Bi<sub>2</sub>W<sub>1-x</sub>Mo<sub>x</sub>O<sub>6</sub>/Montmorillonite nanocomposite as efficient catalyst for photocatalytic desulfurization. *J Alloy Compd* 2017; 709: 285-292. <http://dx.doi.org/10.1016/j.jallcom.2017.03.167>
- [8] Aghabeikzadeh-Naeini E, Movahedi M, Rasouli N and Sadeghi Z. Synthesis of ZnFe<sub>2</sub>O<sub>4</sub> nanoparticles in presence and absence of Tween-20: Optical property, adsorption and photocatalytic activity. *Mat Sci Semicon Proc* 2018; 73: 72-77. <http://dx.doi.org/10.1016/j.mssp.2017.09.024>
- [9] Li FT, Ran JR, Jaroniec M and Qiao SZ. Solution combustion synthesis of metal oxide nanomaterials for energy storage and conversion. *Nanoscale* 2015; 7: 17590-17610. <http://dx.doi.org/10.1039/C5NR05299H>
- [10] Jain SR, Adiga KC and Verneker VRP. A new approach to thermochemical calculations of condensed fuel-oxidizer mixtures. *Combust. Flame* 1981; 40: 71-79. [https://doi.org/10.1016/0010-2180\(81\)90111-5](https://doi.org/10.1016/0010-2180(81)90111-5)
- [11] Patterson AL. The Scherrer formula for X-Ray particle size determination. *Phys Rev* 1939; 56: 978-982. <https://doi.org/10.1103/PhysRev.56.978>

Received on 09-12-2017

Accepted on 19-12-2017

Published on 20-12-2017

DOI: <http://dx.doi.org/10.15377/2409-787X.2017.04.4>

© 2017 Rui-Hong and Fa-Tang; Avanti Publishers.

This is an open access article licensed under the terms of the Creative Commons Attribution Non-Commercial License (<http://creativecommons.org/licenses/by-nc/3.0/>) which permits unrestricted, non-commercial use, distribution and reproduction in any medium, provided the work is properly cited.